# IMPLEMENTATION OF SANC EW CORRECTIONS IN WINHAC MONTE CARLO GENERATOR*

D. Bardin[a,b], S. Bondarenko[c], S. Jadach[a,d], L. Kalinovskaya[a,b]
W. Płaczek[e,a]

[a]H. Niewodniczański Institute of Nuclear Physics, Polish Academy of Sciences
Radzikowskiego 152, 31-342 Kraków, Poland

[b]Dzhelepov Laboratory for Nuclear Problems, JINR
Joliot-Curie 6, 141980 Dubna, Russia

[c]Bogoliubov Laboratory of Theoretical Physics, JINR
Joliot-Curie 6, 141980 Dubna, Russia

[d]CERN, PH Department, 1211 Geneva 23, Switzerland

[e]M. Smoluchowski Institute of Physics, Jagellonian University
Reymonta 4, 30-059 Kraków, Poland

*(Received August 7, 2008)*

In this paper we describe a check of the implementation of `SANC` system generated modules into the framework of the `WINHAC` Monte Carlo event generator. At this stage of work we limit ourselves to inclusion of complete one-loop electroweak corrections to the charged-current Drell–Yan process. We perform tuned comparisons of the results derived with the aid of two codes: (1) the standard `SANC` integrator with YFS-inspired treatment of the ISR QED corrections and (2) the `WINHAC` generator, upgraded with the `SANC` electroweak modules and downgraded to the $\mathcal{O}(\alpha)$ QED corrections. The aim of these comparisons is to prove the correctness of implementation of the `SANC` electroweak modules into the `WINHAC` generator. This is achieved through the presented tuned comparisons.

PACS numbers: 11.15–q, 12.15.–y, 12.15.Lk, 12.20.–m

* This work is partly supported by the EU grant MTKD-CT-2004-510126 in partnership with the CERN Physics Department, by the Polish Ministry of Scientific Research and Information Technology grant No. 620/E-77/6.PR UE/DIE 188/2005-2008, by the EU Marie Curie Research Training Network grant under the contract No. MRTN-CT-2006-035505 and by the Russian Foundation for Basic Research grant No. 07-02-00932.

## 1. Introduction

The main aim of this work is to implement in the Monte Carlo (MC) event generator WINHAC [1] the complete $\mathcal{O}(\alpha)$ electroweak (EW) corrections delivered by the SANC system in the form of the Standard SANC FORTRAN Modules (SSFM) automatically generated by the system and to perform a cross check of this implementation by means of tuned comparisons of a few distributions with simple cuts. Here we limit ourselves to the charged current Drell–Yan-like single $W$ production and use the setup which is rooted in the convention of TeV4LHC WS tuned comparisons working group, see Ref. [2]

$$pp \longrightarrow W^+ + X \longrightarrow \ell^+\nu_\ell + X\,. \tag{1.1}$$

For the description of WINHAC and SANC we refer the reader to the literature: for WINHAC to [3] and for SANC to [4] and to [5][1].

For the case of the charged current (CC) and neutral current (NC) Drell–Yan (DY) processes an extended description of the SANC approach can be found in Refs. [6] and [7], correspondingly.

For the final state QED radiative corrections WINHAC has been compared with the Monte Carlo generator HORACE, both for the parton-level processes and for proton–proton collisions at the LHC. Good agreement of the two programs for several observables has been found [8]. The comparisons with generator PHOTOS also show good agreement of the two generators for the QED final state radiation (FSR) [9].

A similar event generator for the $Z$ boson production, called ZINHAC, is under development now. Krakow group also works on constrained MC algorithms for the QCD ISR parton shower that could be applied to Drell–Yan processes, see *e.g.* Ref. [10].

Many results of tuned comparison of SANC with several other programs were presented for CC case in Ref. [11] and [2] and for NC case in [12], showing very good agreement. This ensures us in a high confidence of NLO EW SANC predictions.

In this paper we limit ourselves to presenting the numerical tests of the implementation of SANC EW corrections in generator WINHAC, detailed description of the implementation itself will be given elsewhere. The paper is organized as follows. In Section 2 we describe the setup of the tuned comparisons between SANC and WINHAC. In Section 3 we present the results of these comparisons for the total cross-sections and various distributions, first at the Born level then for $\mathcal{O}(\alpha)$ EW corrections, and finally for a model of purely weak corrections. Finally, Section 4 concludes the paper.

[1] SANC is available from the project homepages at Dubna http://sanc.jinr.ru and CERN http://pcphsanc.cern.ch

## 2. Setup of tuned comparisons of SANC and WINHAC

We use the input parameter set as in Ref. [2], see also comments after Eq. (4.4.37)

$$\begin{aligned}
G_\mu &= 1.16637\times10^{-5}\mathrm{GeV}^{-2}, \quad \alpha=1/137.03599911\,,\ \alpha_{\rm s}(M_Z^2)=0.1176\,,\\
M_Z &= 91.1876\mathrm{GeV}\,, \qquad \Gamma_Z = 2.4924\mathrm{GeV}\,,\\
M_W &= 80.37399\mathrm{GeV}\,, \qquad \Gamma_W = 2.0836\mathrm{GeV}\,,\\
M_H &= 115\mathrm{GeV}\,,\\
m_e &= 0.51099892\mathrm{MeV}\,, \qquad m_\mu = 0.105658369\mathrm{GeV}\,,\\
m_\tau &= 1.77699\mathrm{GeV}\,,\\
m_u &= 0.06983\mathrm{GeV}\,, \qquad m_c = 1.2\mathrm{GeV}\,,\ m_t = 174\mathrm{GeV}\,,\\
m_d &= 0.06984\mathrm{GeV}\,, \qquad m_s = 0.15\mathrm{GeV}\,,\ m_b = 4.6\mathrm{GeV}\,,\\
|V_{ud}| &= 0.975, \quad |V_{us}| = 0.222\,,\\
|V_{cd}| &= 0.222, \quad |V_{cs}| = 0.975\,,\\
|V_{cb}| &= |V_{ts}| = |V_{ub}| = |V_{td}| = |V_{tb}| = 0\,.
\end{aligned} \tag{2.1}$$

However, we present the results both in the $\alpha(0)$ and $G_\mu$ one-loop parametrization schemes. Explicit QCD corrections are not included in our calculations.

To compute the hadronic cross-section we also use the MRST2004QED set of parton density functions [13], and take the renormalization scale, $\mu_{\rm r}$, and the QED and QCD factorization scales, $\mu_{\rm QED}$ and $\mu_{\rm QCD}$, to be $\mu_{\rm r}^2 = \mu_{\rm QED}^2 = \mu_{\rm QCD}^2 = M_W^2$.

We impose only detector acceptance cuts on the leptons transverse momenta and the charged lepton pseudorapidity ($\eta_\ell$)

$$p_{\rm T}^\ell > 20\,\mathrm{GeV}\,, \qquad |\eta(\ell)| \ < \ 2.5\,, \qquad \ell = e,\mu\,, \tag{2.2}$$

$$\not{p}_{\rm T}^{\,\nu} \ > \ 20\ \mathrm{GeV}\,, \tag{2.3}$$

where $\not{p}_{\rm T}^{\,\nu}$ is the missing transverse momentum originating from the neutrino.

To simplify the conditions of this purely technical comparison, we do not impose lepton identification requirements, as given in Table 4.4.49 of Ref. [2], so we provide "simplified bare" results, *i.e.* without smearing, recombination and lepton separation cuts. We present our results only for three differential distributions and the total cross-sections, at LO and NLO, and the corresponding relative corrections, $\delta_{\rm EW}\,[\%] = d\sigma_{\rm NLO}/d\sigma_{\rm LO} - 1$, for two processes: $pp \to W^+ + X \to \ell^+\nu_\ell + X$ with $\ell = e,\ \mu$ at the LHC in two schemes: $\alpha(0)$ and $G_\mu$. Moreover, we present the results for some well-defined model of "purely weak" corrections $\delta_{\rm weak}$, given in Subsection 3.2.3, for the same cases as for $\delta_{\rm EW}$.

In our comparisons we use the following *W-boson observables*:

- $\sigma_W$: the *total inclusive cross-section* of the $W$-boson production;
- $\dfrac{d\sigma}{dM_{\rm T}^{\rm W}}$: the *transverse mass* distribution of the lepton lepton–neutrino pair. The transverse mass is defined as

$$M_{\rm T}^{\rm W} = \sqrt{2p_{\rm T}^{\ell}p_{\rm T}^{\nu}(1-\cos\phi^{\ell\nu})}\,, \tag{2.4}$$

  where $p_{\rm T}^{\nu}$ is the transverse momentum of the neutrino, and $\phi^{\ell\nu}$ is the angle between the charged lepton and the neutrino in the transverse plane. The neutrino transverse momentum is identified with the missing transverse momentum, $\not{p}_{\rm T}$, in the event;
- $\dfrac{d\sigma}{dp_{\rm T}^{\ell}}$: the *transverse lepton momentum* distribution;
- $\dfrac{d\sigma}{d|\eta_\ell|}$: the *lepton pseudorapidity* distribution

$$\eta_\ell = -\ln\left(\tan\frac{\theta_\ell}{2}\right)\,. \tag{2.5}$$

  where the lepton kinematical variables are defined in the laboratory frame.

One should emphasize an important difference between the conditions of these comparisons and that of TeV4LHC WS concerning the subtraction of initial quark mass singularities. Instead of the commonly adopted $\overline{\rm MS}$ or DIS subtraction scheme (as, for example, in Ref. [2]), we use here an YFS-inspired subtraction method [14].

$$d\sigma_{\rm ISR}^{\rm YFS}(\hat{s},m_d,m_u;\epsilon) = d\sigma_{\rm ISR}^{\rm Born}(\hat{s},m_d,m_u;\epsilon)\,\delta_{\rm ISR}^{\rm YFS}(\hat{s},m_d,m_u;\epsilon)\,, \tag{2.6}$$

where

$$\begin{aligned}\delta_{\rm ISR}^{\rm YFS}(\hat{s},m_d,m_u;\epsilon) \;=\; & \frac{\alpha}{\pi}\Bigg\{\left[Q_d^2\left(\ln\frac{\hat{s}}{m_d^2}-1\right)+Q_u^2\left(\ln\frac{\hat{s}}{m_u^2}-1\right)-1\right]\ln\epsilon \\ & + Q_d^2\left(\frac{3}{4}\ln\frac{\hat{s}}{m_d^2}-1+\frac{\pi^2}{6}\right) \\ & + Q_u^2\left(\frac{3}{4}\ln\frac{\hat{s}}{m_u^2}-1+\frac{\pi^2}{6}\right)+1-\frac{\pi^2}{3}\Bigg\}\,,\end{aligned} \tag{2.7}$$

with

$$\epsilon = \frac{2\omega}{\sqrt{\hat{s}}}\,, \tag{2.8}$$

being the dimensionless soft–hard photon separator ($\omega$ is the photon energy). The $Q_u$, $Q_d$ are the electric charges of the up-type and down-type quarks in the units of the positron charge and $m_u$, $m_d$ are their masses, while $\hat{s}$ is the centre-of-mass energy squared of the incoming quarks.

Simultaneously, we subtract in a gauge-invariant way the contribution of the ISR hard photons, derived using the $W$ propagator splitting technique [15]. In this way the initial quark mass dependence drops out from the one-loop level observables.

In order to define our "weak" corrections, we will need the YFS corrections for the "initial-final" interference

$$\begin{aligned}\delta^{\rm YFS}_{\rm Int}(\hat{s},t,u;\epsilon) \;=\; & \frac{\alpha}{\pi}\Bigg\{2\left[Q_d\ln\frac{\hat{s}}{-t}-Q_u\ln\frac{\hat{s}}{-u}+1\right]\ln\frac{M_W^2\,\epsilon}{\sqrt{\left(s-M_W^2\right)^2+M_W^2\Gamma_W^2}}\\ & +\; Q_d\left[\frac{1}{2}\ln\frac{\hat{s}}{-t}\left(\ln\frac{\hat{s}}{-t}+1\right)+{\rm Li}_2\left(1+\frac{\hat{s}}{t}\right)\right]\\ & -\; Q_u\left[\frac{1}{2}\ln\frac{\hat{s}}{-u}\left(\ln\frac{\hat{s}}{-u}+1\right)+{\rm Li}_2\left(1+\frac{\hat{s}}{u}\right)\right]+\frac{\pi^2}{6}-2\Bigg\}\,,\end{aligned} \tag{2.9}$$

and for the "final state radiation"

$$\delta^{\rm YFS}_{\rm FSR}(\hat{s},m_l;\epsilon) \;=\; \frac{\alpha}{\pi}\left\{\left(\ln\frac{\hat{s}}{m_l^2}-2\right)\ln\epsilon+\frac{3}{4}\ln\frac{\hat{s}}{m_l^2}-\frac{\pi^2}{6}\right\}, \tag{2.10}$$

where $\hat{s}$, $t$, $u$ are the standard Mandelstam variables for the parton-level process and $m_l$ is the charged lepton mass.

## 3. Numerical results

In this section we present the numerical results of the tuned comparisons between `SANC` and `WINHAC`, first the the Born level (LO) and then including the $\mathcal{O}(\alpha)$ EW corrections (NLO). At the end of this section we compare also the so-called "purely weak" corrections which are the difference between the EW corrections and the "QED" corrections defined by the terms given in Eqs. (2.9), (2.10) plus the corresponding hard-photon contributions.

### *3.1. Comparisons at tree level, LO*

We begin with the comparisons at the Born level. In Figs. 1–3 the distributions are shown for all three observables under consideration only for $\mu^+$ final state but in the both schemes: $\alpha(0)$ and $G_\mu$. The lower parts

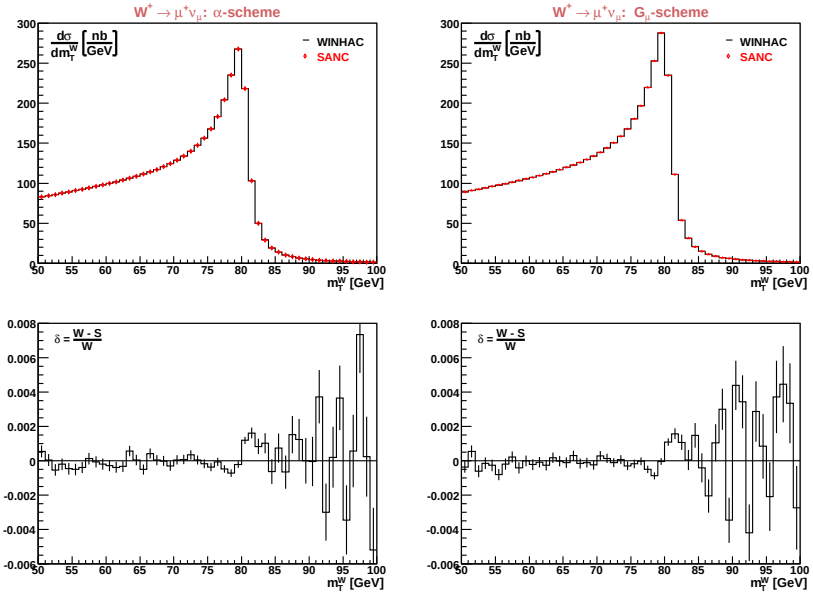


Fig. 1. The Born distributions of $M_{\mathrm{T}}^{\mathrm{W}}$ from SANC (red diamonds) and WINHAC (solid lines) in two schemes and their relative deviations $\delta = (\mathrm{W} - \mathrm{S})/\mathrm{W}$.

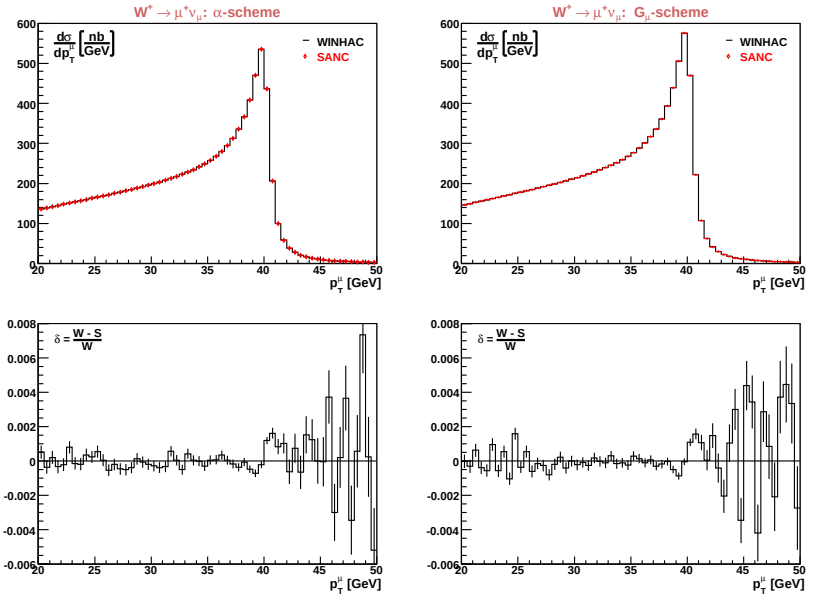


Fig. 2. The Born distributions of $p_{\mathrm{T}}^{\ell}$ from SANC (red diamonds) and WINHAC (solid lines) in two schemes and their relative deviations $\delta = (\mathrm{W} - \mathrm{S})/\mathrm{W}$.

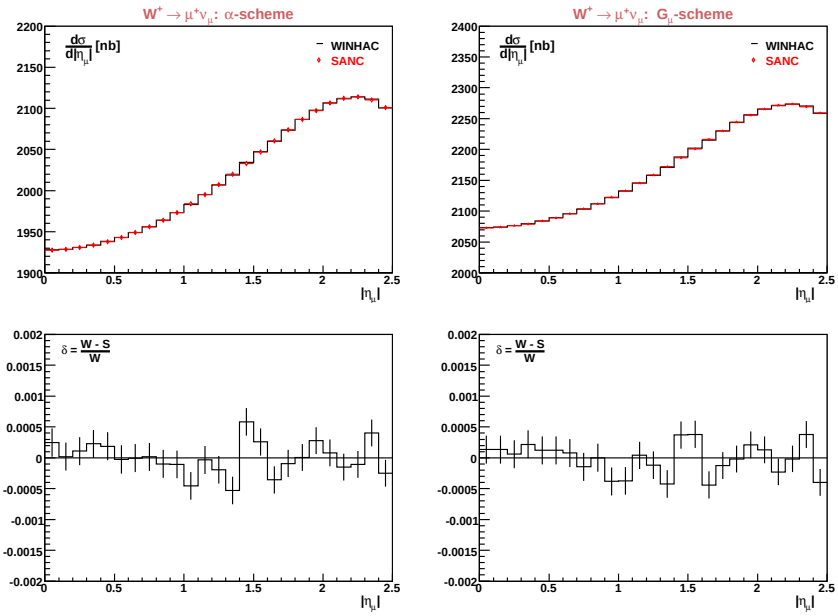


Fig. 3. The Born distributions of $|\eta_\ell|$ from SANC (red diamonds) and WINHAC (solid lines) in two schemes and their relative deviations $\delta = (\mathrm{W} - \mathrm{S})/\mathrm{W}$.

of the figures shows the relative deviation $\Delta = (\mathrm{W} - \mathrm{S})/\mathrm{W}$ between the two calculations (W for WINHAC, S for SANC).

As seen, the relative deviations lie within the 1 per-mill band, wherever the cross-section is not very small[2]. We do not show the comparisons for electron channel, since at tree level the muon mass effects are negligible, and the plots look identical.

### *3.2. Comparison at one-loop level, NLO inclusive cross-sections*

Turning to the NLO results, we show, first of all, in Table I the comparisons of the inclusive cross-sections (in pb) within the acceptance cuts and the relative radiative correction factor (in %), as seen by two calculations (second and third rows). In the first row we show SANC results in the conditions of TeV4LHC WS. The numbers agree with those published in [2] within statistical errors.

The Born cross-sections from SANC and WINHAC agree well within statistical errors ($< 10^{-4}$). The EW NLO cross-sections agree not worse than within a half a per mill or agree even within statistical errors in both schemes, both

[2] On the SANC side we have both a VEGAS [16] based integrator and a FOAM [17] based event generator. In this comparison the integrator has been used.

for the electron and muon channels, better for the muon channel where we observe the agreement within the statistical errors.

TABLE I

The tuned comparisons of the LO and EW NLO predictions for $\sigma_W$ and $\delta_{\rm EW}$ from SANC and WINHAC for the simplified bare cuts. The statistical errors of the Monte Carlo integration are given in parentheses.

| **LHC,** $pp \to W^+ + X \to e^+\nu_e + X$ | | | | | | |
|---|---|---|---|---|---|---|
| | $\alpha$-scheme | | | $G_\mu$-scheme | | |
| | LO [pb] | NLO [pb] | $\delta_{\rm EW}$ [%] | LO [pb] | NLO [pb] | $\delta_{\rm EW}$ [%] |
| SANC-$\overline{\rm MS}$ | 5039.19(2) | 5139.33(5) | 1.987(1) | — | — | — |
| SANC-YFS | 5039.19(2) | 5137.53(3) | 1.952(1) | 5419.18(2) | 5208.48(3) | −3.888(1) |
| WINHAC | 5039.06(11) | 5138.04(16) | 1.966(3) | 5419.04(12) | 5209.04(12) | −3.874(3) |

| **LHC,** $pp \to W^+ + X \to \mu^+\nu_\mu + X$ | | | | | | |
|---|---|---|---|---|---|---|
| | $\alpha$-scheme | | | $G_\mu$-scheme | | |
| | LO [pb] | NLO [pb] | $\delta_{\rm EW}$ [%] | LO [pb] | NLO [pb] | $\delta_{\rm EW}$ [%] |
| SANC-$\overline{\rm MS}$ | 5039.20(2) | 5229.58(6) | 3.778(1) | — | — | — |
| SANC-YFS | 5039.20(2) | 5227.73(2) | 3.741(1) | 5419.19(2) | 5305.47(3) | −2.098(1) |
| WINHAC | 5039.03(11) | 5227.87(14) | 3.745(2) | 5419.01(12) | 5305.59(14) | −2.094(2) |

#### 3.2.1. NLO distributions: electron channel

We begin the comparisons of the distributions for the electron channel in two schemes for our three $W$ observables ($M_{\rm T}^{\rm W}, p_{\rm T}^{\ell}$ and $|\eta_\ell|$, Figs. 4–6, correspondingly) with the "simplified bare" cuts. The two upper figures show the quantity $\delta_{\rm EW}$ in %, while the two lower figures show absolute deviations $\Delta = {\rm W} - {\rm S}$ between the two calculations.

As seen, the $\mathcal{O}(\alpha)$ EW correction $\delta_{\rm EW}$ is quite large (mainly due to the FSR QED contribution), it varies by 18% depending on the scheme. It is shifted to the larger negative values in the $G_\mu$ scheme and more moderate in the $\alpha(0)$ scheme, the reason for which the latter was preferred by tuned group of TeV4LHC WS. The absolute deviation for both schemes does not exceed 0.1% in the important regions where the cross-section is large.

For the $p_{\rm T}^e$ distributions, it varies within 25% but this is an artificial result of applying "simplified bare" cuts. The $\eta_\ell$ distributions are flat and show little biases of the order of a quarter of a per mill. However, most likely VEGAS errors are underestimated in the SANC results.

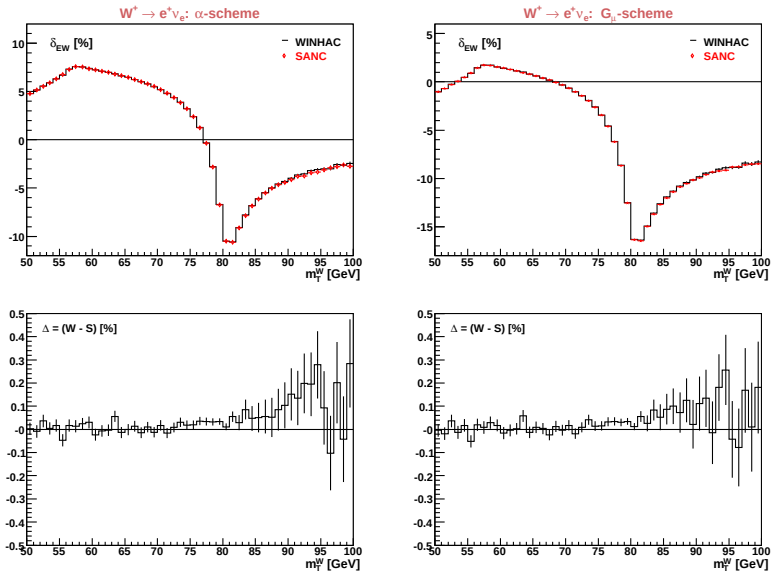


Fig. 4. The EW NLO distributions of $M_{\mathrm{T}}^{\mathrm{W}}$ from `SANC` (red diamonds) and `WINHAC` (solid lines) for the electron channel in two schemes and their absolute deviations $\Delta = \mathrm{W} - \mathrm{S}$.

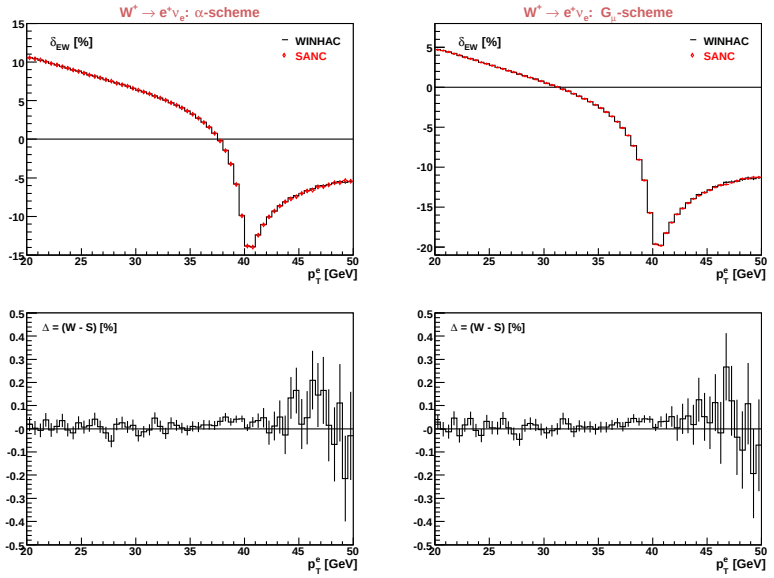


Fig. 5. The EW NLO distributions of $p_{\mathrm{T}}^{\ell}$ from `SANC` (red diamonds) and `WINHAC` (solid lines) for the electron channel in two schemes and their absolute deviations $\Delta = \mathrm{W} - \mathrm{S}$.

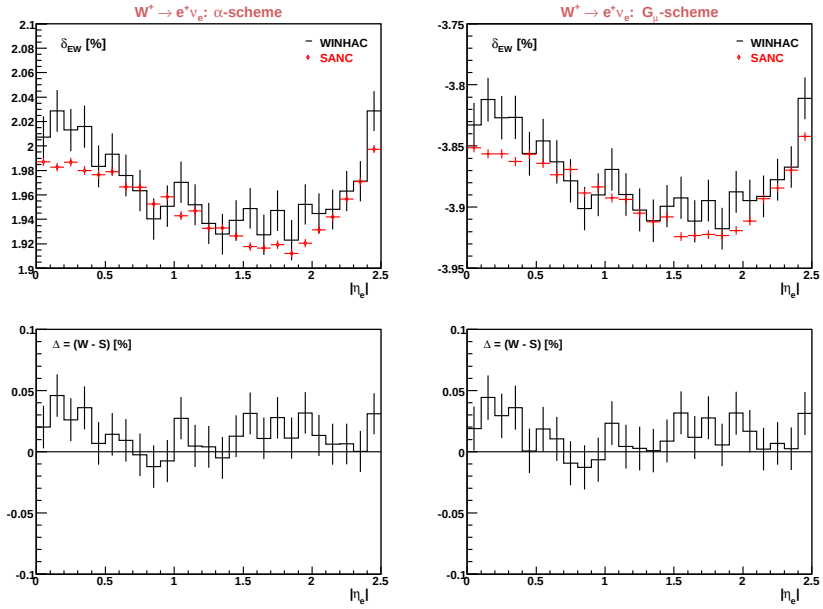


Fig. 6. The EW NLO distributions of $|\eta_\ell|$ from `SANC` (red diamonds) and `WINHAC` (solid lines) for the electron channel in two schemes and their absolute deviations $\Delta = \mathrm{W} - \mathrm{S}$.

### 3.2.2. NLO distributions: muon channel

We continue the comparisons for muon channels in two schemes for the same three $W$ observables ($M_{\mathrm{T}}^{\mathrm{W}}, p_{\mathrm{T}}^{\ell}$ and $|\eta_\ell|$) with the "simplified bare" cuts. The results are presented in Figs. 7–9, respectively. Again, the two upper figures show EW NLO correction $\delta_{\mathrm{EW}}$ in %, and the two lower figures show absolute deviations W−S between the two calculations. Here the absolute deviations in statistically saturated regions do not exceed 0.05% and in average is of the order of 0.025%. For the muon channel both calculations are statistical consistent and no evident biases are observed. It is important to emphasis that biases could be present, in principle, due to finite muon mass, which treatment in two calculations is not identical: for the muon channel `SANC` uses fully massive formulae for all contributions while `WINHAC` uses a mixed approach — electroweak virtual and soft real-photon corrections are calculated in the massless fermion approximation, while massive fermions are kept in hard real-photon radiation.

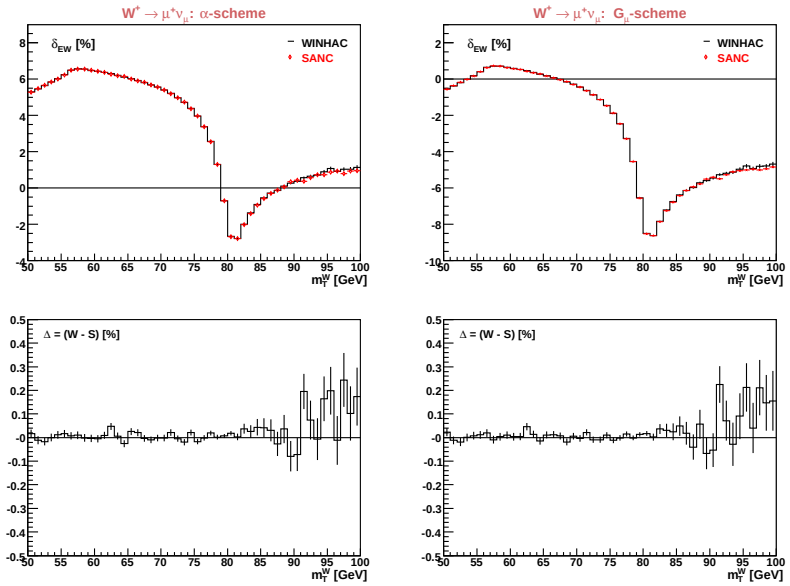


Fig. 7. The EW NLO distributions of $M_{\mathrm{T}}^{\mathrm{W}}$ from `SANC` (red diamonds) and `WINHAC` (solid lines) for the muon channel in two schemes and their absolute deviations $\Delta = \mathrm{W} - \mathrm{S}$.

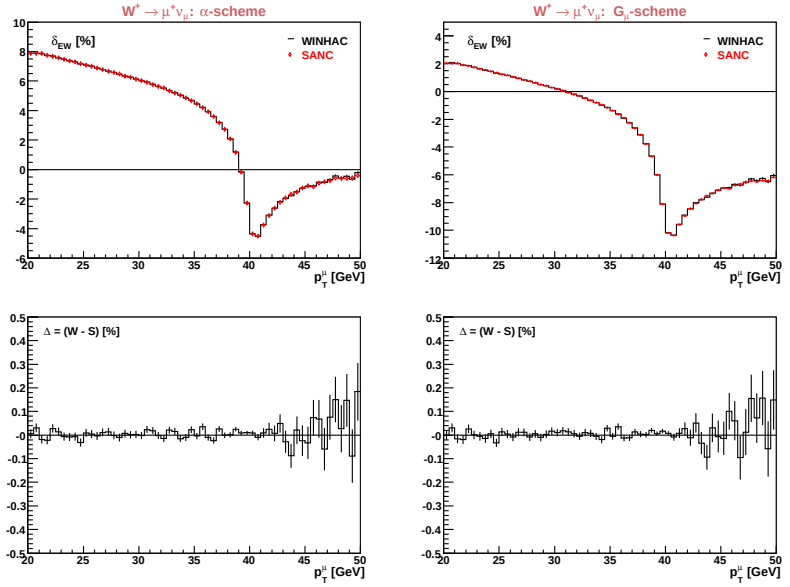


Fig. 8. The EW NLO distributions of $p_{\mathrm{T}}^{\ell}$ from `SANC` (red diamonds) and `WINHAC` (solid lines) for the muon channel in two schemes and their absolute deviations $\Delta = \mathrm{W} - \mathrm{S}$.

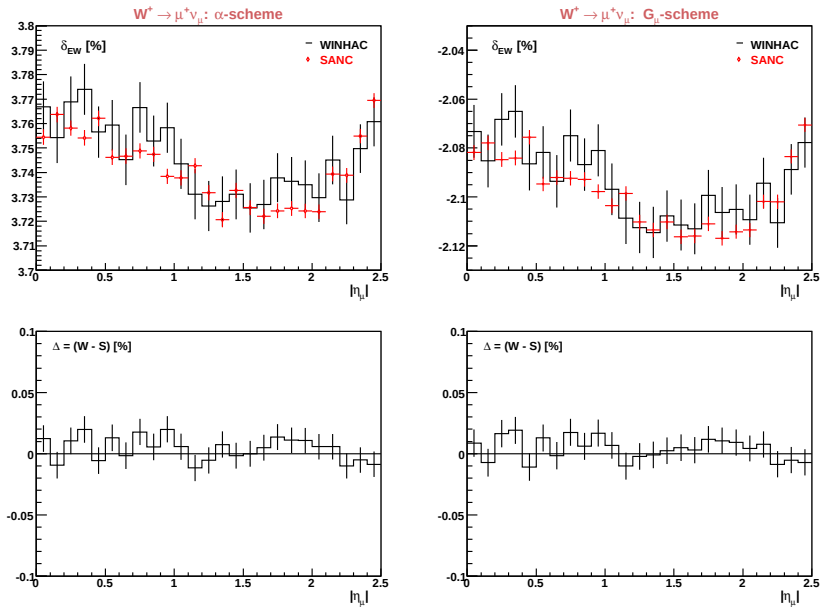


Fig. 9. The EW NLO distribution of $|\eta_\ell|$ from SANC (red diamonds) and WINHAC (solid lines) for the muon channel in two schemes and their absolute deviations $\Delta = \mathrm{W} - \mathrm{S}$.

### 3.2.3. Weak corrections

Here we discuss the "purely weak" corrections which are defined as

$$\delta_{\rm weak} \;=\; \delta^{\rm EW}_{\rm softvirt} \;-\; \delta^{\rm YFS}_{\rm softvirt}\,, \tag{3.1}$$

where

$$\delta^{\rm YFS}_{\rm softvirt} \;=\; \delta^{\rm YFS}_{\rm ISR} \;+\; \delta^{\rm YFS}_{\rm Int} \;+\; \delta^{\rm YFS}_{\rm FSR}\,, \tag{3.2}$$

with three contributions given by Eqs. (2.7)–(2.10). The contribution $\delta^{\rm EW}_{\rm softvirt}$ includes the 1-loop EW corrections plus the real soft-photon correction and is provided by the SANC modules. This definition is free of any regularization scales.

From Table II one sees, that for the electron channel the agreement is very good, while for the muon channel we observe the systematic differences of about 0.007%. This can be attributed to different treatment of the muon mass in the two programs: SANC uses the fully massive formulae while WINHAC uses the massless-lepton approximation for these corrections. The "weak" corrections in the $\alpha$-scheme are quite sizable, $\sim 6\%$, because of

the light-fermion loop contributions, $\sim \ln(\hat{s}/m_f^2)$, to the $W$ self-energy correction. Such contributions drop out in the $G_\mu$-scheme making the "weak" corrections much smaller, $\sim 0.1\%$. In Figs. 10–15 we show the distributions

TABLE II

The tuned comparisons of the "purely weak" corrections $\delta_{\rm weak}$ from SANC and WINHAC for the simplified bare cuts. The statistical errors of the Monte Carlo integration are given in parentheses.

| $\delta_{\rm weak}$ [%] | | |
|---|---|---|
| **LHC,** $pp \to W^+ + X \to e^+\nu_e + X$ | | |
| | $\alpha$-scheme | $G_\mu$-scheme |
| SANC | 5.7223(2) | −0.1175(2) |
| WINHAC | 5.7220(3) | −0.1177(0) |

| **LHC,** $pp \to W^+ + X \to \mu^+\nu_\mu + X$ | | |
|---|---|---|
| | $\alpha$-scheme | $G_\mu$-scheme |
| SANC | 5.7286(2) | −0.1109(2) |
| WINHAC | 5.7220(2) | −0.1177(0) |

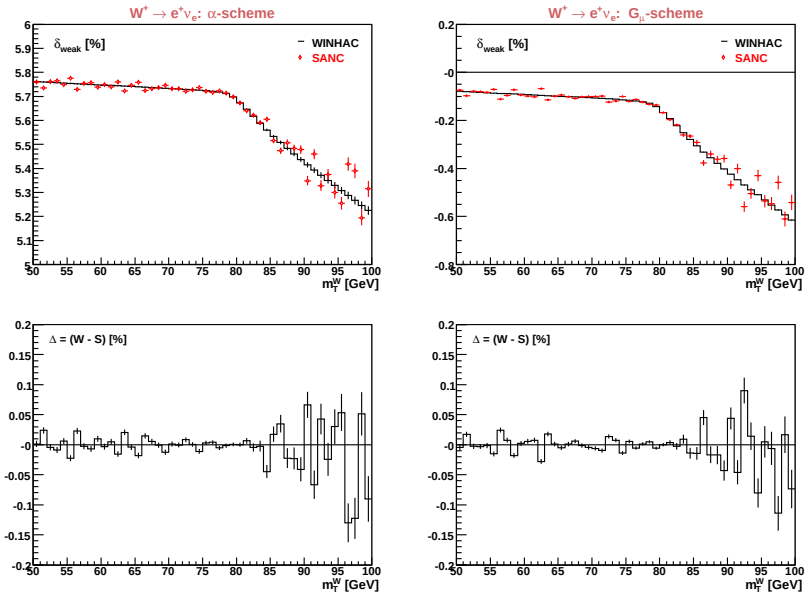


Fig. 10. The "weak" correction distributions of $M_{\rm T}^{\rm W}$ from SANC (red diamonds) and WINHAC (solid lines) for the electron channel in two schemes and their absolute deviations $\Delta = {\rm W} - {\rm S}$.

of the "weak" corrections and absolute deviations between the two calculations. The figures show agreement at the level 0.01%. In some cases the biases of the same order are seen. Again, this might be a consequence of underestimation of errors by VEGAS. In the muon channel, the observed deviations at the level of 0.01% can be attributed again to different treatment of the muon mass in the two programs.

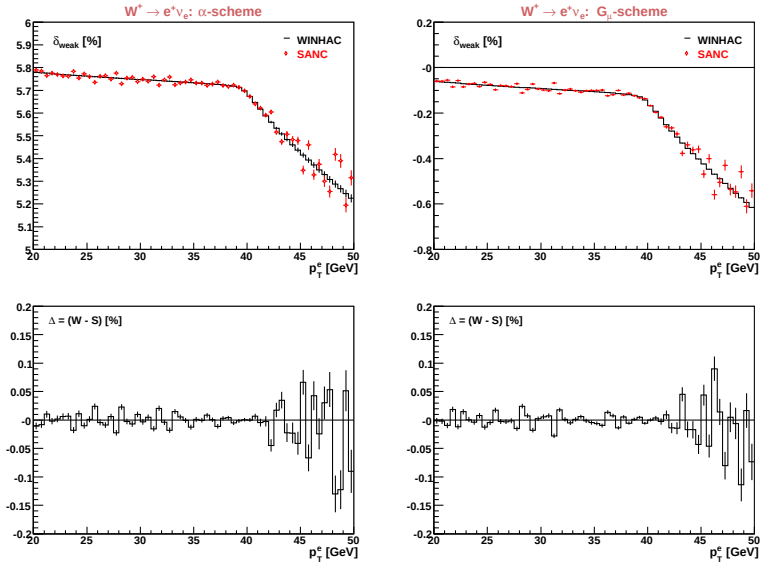


Fig. 11. The "weak" correction distributions of $p_{\mathrm{T}}^{\ell}$ from SANC (red diamonds) and WINHAC (solid lines) for the electron channel in two schemes and their absolute deviations $\Delta = \mathrm{W} - \mathrm{S}$.

## 4. Conclusions

The main priority of the development of SANC as a HEP tool for the LHC is to create the Standard SANC FORTRAN Modules (SSFM) for the electroweak corrections at one-loop level to be used in existing MC event generators.

The goals of this work were: (a) to integrate the charged-current Drell–Yan SSFM into the Monte Carlo event generator WINHAC and (b) to check thoroughly the stability of numbers for simple distributions by comparisons of the WINHAC generated results with those provided by the recently created SANC charged-current Drell–Yan integrator. In this paper we have concentrated on presenting the numerical tests of the implementation of the above electroweak corrections in WINHAC, while the details on this implementation will be given elsewhere.

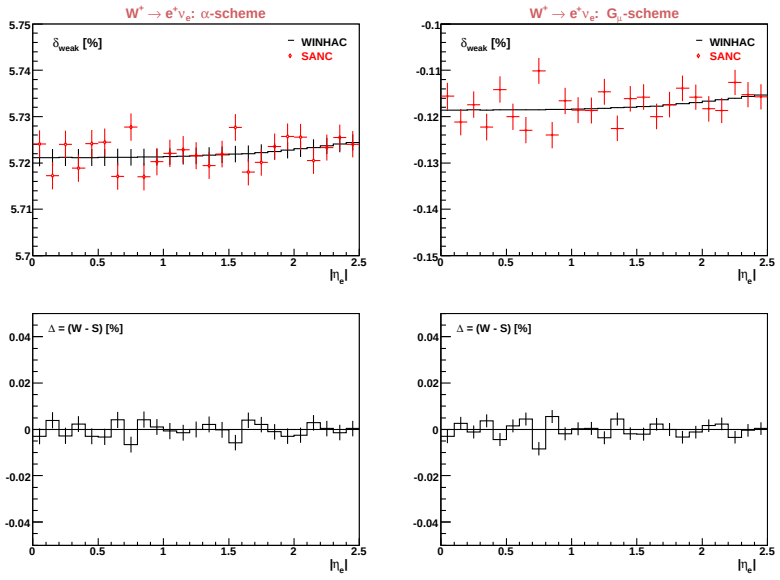


Fig. 12. The "weak" correction distributions of $|\eta_\ell|$ from `SANC` (red diamonds) and `WINHAC` (solid lines) for the electron channel in two schemes and their absolute deviations $\Delta = \mathrm{W} - \mathrm{S}$.

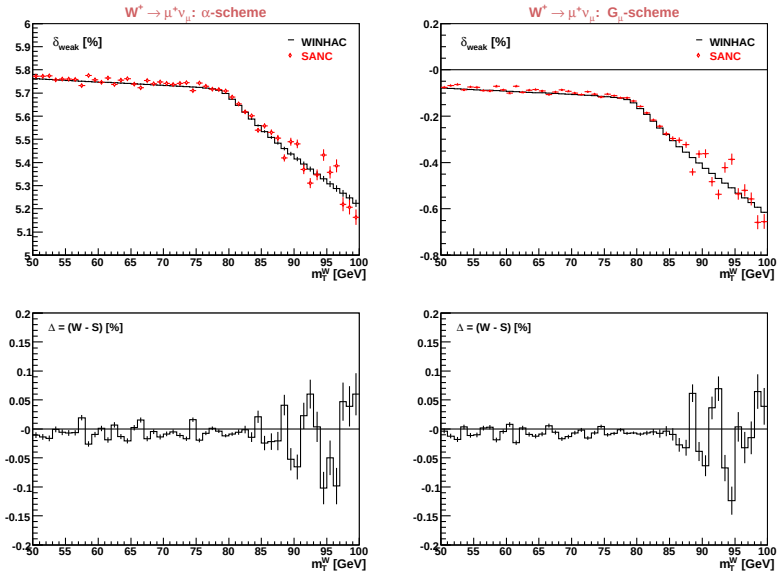


Fig. 13. The "weak" correction distributions of $M_{\mathrm{T}}^{\mathrm{W}}$ from `SANC` (red diamonds) and `WINHAC` (solid lines) for the muon channel in two schemes and their absolute deviations $\Delta = \mathrm{W} - \mathrm{S}$.

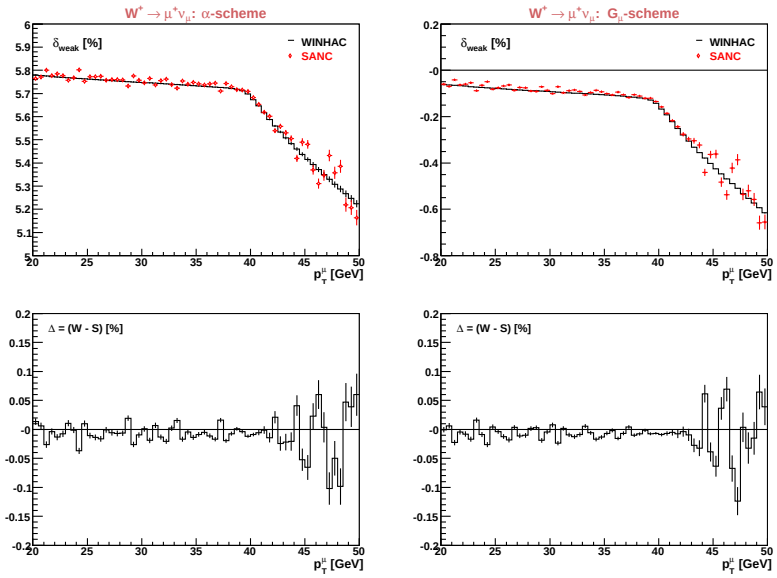


Fig. 14. The "weak" correction distributions of $p_{\mathrm{T}}^{\ell}$ from SANC (red diamonds) and WINHAC (solid lines) for the muon channel in two schemes and their absolute deviations $\Delta = \mathrm{W} - \mathrm{S}$.

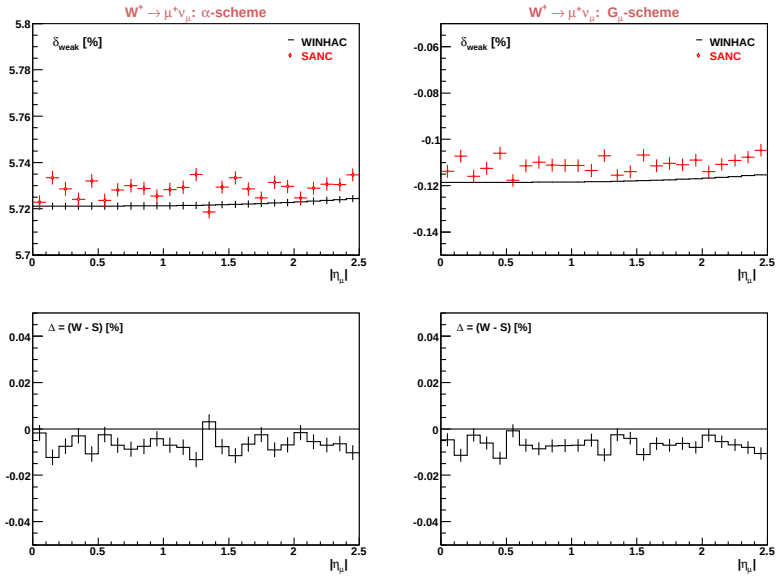


Fig. 15. The "weak" correction distributions of $|\eta_{\ell}|$ from SANC (red diamonds) and WINHAC (solid lines) for the muon channel in two schemes and the absolute deviations $\Delta = \mathrm{W} - \mathrm{S}$.

The main and very important conclusion of this paper is that we have reached the agreement between the `WINHAC` MC event generator and the `SANC` MC integrator for the $\mathcal{O}(\alpha)$ electroweak corrections to the charged-current Drell–Yan process at the sub-per-mill level, both for the inclusive cross-section and for the main distributions. Thus, our above goals have been achieved.

Another important conclusion is that the MC event generator `WINHAC` can now be used for precision simulations of the charged-current Drell–Yan process at the LHC including the $\mathcal{O}(\alpha)$ electroweak corrections. It can also serve as a benchmark for testing other MC programs for this process.

The next step on this road would be a similar implementation of the `SANC` modules in the neutral-current Drell–Yan MC event generator `ZINHAC`, being under development now.

The authors are grateful to A. Arbuzov, P. Christova and R. Sadykov for numerous discussions of related issues. Two of us (D.B. and L.K.) are cordially indebted to S. Jadach and Z. Wąs for offering us an opportunity of encouraging common work with scientists of Institute of Nuclear Physics, Kraków in May–June 2008 and to the Institute of Nuclear Physics directorate for hospitality which was extended to us in this period, when the major part of this study was done. We also acknowledge the hospitality of the CERN PH Theory Unit where this work was finalized.

## REFERENCES

[1] W. Płaczek, S. Jadach, WINHAC: The Monte Carlo Event Generator for Single $W$-Boson Production with Leptonic Decays in Hadron Collisions, available from `http://cern.ch/placzek/winhac`

[2] C.E. Gerber *et al.*, `0705.3251 [hep-ph]`.

[3] W. Płaczek, S. Jadach, *Eur. Phys. J.* **C29**, 325 (2003) [`hep-ph/0302065`].

[4] A. Andonov *et al.*, *Comput. Phys. Commun.* **174**, 481 (2006) [`hep-ph/0411186`].

[5] D. Bardin *et al.*, *Comput. Phys. Commun.* **177**, 738 (2007) [`hep-ph/0506120`].

[6] A. Arbuzov *et al.*, *Eur. Phys. J.* **C46**, 407 (2006) [`hep-ph/0506110`].

[7] A. Arbuzov *et al.*, *Eur. Phys. J.* **C54**, 451 (2008) [`0711.0625 [hep-ph]`].

[8] C.M. Carloni Calame *et al.*, *Acta Phys. Pol. B* **35**, 1643 (2004) [`hep-ph/0402235`].

[9] P. Golonka, Z. Was, *Eur. Phys. J.* **C45**, 97 (2006) [`hep-ph/0506026`].

[10] S. Jadach *et al.*, Report FJPAN-IV-2007-3, CERN-PH-TH/2007-059; submitted to *Comput. Phys. Commun.*, `hep-ph/0703281`.

[11] C. Buttar *et al.*, hep-ph/0604120.

[12] C. Buttar *et al.*, 0803.0678 [hep-ph].

[13] A. D. Martin *et al.*, *Eur. Phys. J.* **C39**, 155 (2005) [hep-ph/0411040].

[14] D. Wackeroth, W. Hollik, *Phys. Rev.* **D55**, 6788 (1997) [hep-ph/9606398].

[15] F A. Berends *et al.*, *Z. Phys.* **C27**, 155 (1985).

[16] G.P. Lepage, *J. Comput. Phys.* **27**, 192 (1978).

[17] S. Jadach, P. Sawicki, *Comput. Phys. Commun.* **177**, 441 (2007) [physics/0506084].